



TITLE:

Exploring metameric variation in human molars: A morphological study using morphometric mapping

AUTHOR(S):

Morita, Wataru; Morimoto, Naoki; Ohshima, Hayato

CITATION:

Morita, Wataru ...[et al]. Exploring metameric variation in human molars: A morphological study using morphometric mapping. *Journal of Anatomy* 2016, 229(3): 343-355

ISSUE DATE:

2016-09

URL:

<http://hdl.handle.net/2433/230210>

RIGHT:

This is the peer reviewed version of the following article: [Wataru Morita Naoki Morimoto Hayato Ohshima. Exploring metameric variation in human molars: a morphological study using morphometric mapping.], which has been published in final form at <http://dx.doi.org/10.1111/joa.12482>. This article may be used for non-commercial purposes in accordance with Wiley Terms and Conditions for Self-Archiving.; The full-text file will be made open to the public on 05 August 2017 in accordance with publisher's 'Terms and Conditions for Self-Archiving'; この論文は出版社版でありません。引用の際には出版社版をご確認ください。; This is not the published version. Please cite only the published version.

Original Paper

Title: Exploring metameric variation in human molars: a morphological study using morphometric mapping

Wataru Morita^{1,2†}, Naoki Morimoto^{3†}, and Hayato Ohshima^{2*}

¹Department of Oral Functional Anatomy, Hokkaido University Graduate School of Dental Medicine, Sapporo, Japan

²Division of Anatomy and Cell Biology of the Hard Tissue, Department of Tissue Regeneration and Reconstruction, Niigata University Graduate School of Medical and Dental Sciences, Niigata, Japan

³Laboratory of Physical Anthropology, Department of Zoology, Graduate School of Science, Kyoto University, Kyoto, Japan

Running headline: Metameric variation in human molars

[†]Contributed equally to this work with: Wataru Morita, Naoki Morimoto

^{*}Corresponding author:

Hayato Ohshima, DDS, PhD

Division of Anatomy and Cell Biology of the Hard Tissue, Department of Tissue Regeneration and Reconstruction, Niigata University Graduate School of Medical and Dental Sciences, 2-5274 Gakkocho-dori, Chuo-ku, Niigata 951-8514, Japan

TEL +81-25-227-2812

FAX +81-25-227-0804

E-mail: histoman@dent.niigata-u.ac.jp

Abstract

Human molars exhibit a type of metameric variation, which is the difference in serially repeated morphology within an organism. Various theories have been proposed to explain how this variation is brought about in the molars. Actualistic data that support the theories, however, are still relatively scarce because of methodological limitations. Here we propose new methods to analyze detailed tooth crown morphologies. We applied morphometric mapping to the enamel–dentine junction of human maxillary molars and examined whether odontogenetic models were adaptable to human maxillary molars. Our results showed that the upper first molar is phenotypically distinct among the maxillary molars. The average shape of the upper first molar is characterized by four well-defined cusps and precipitous surface relief of the occlusal table. On the other hand, upper third molar is characterized by smooth surface relief of the occlusal table and shows greater shape variation and distinct distribution patterns in morphospace. The upper second molar represents an intermediate state between first and third molar. Size-related shape variation was investigated by the allometric vector analysis, and it appeared that human maxillary molars tend to converge toward the shape of the upper first molar as the size increases. Differences between the upper first molar versus second and third molar can thus be largely explained as an effect of allometry. Collectively, these results indicate that the observed pattern of metameric variation in human molars is consistent with odontogenetic models of molar row structure (inhibitory cascade model) and molar crown morphology (patterning cascade model). This study shows that morphometric mapping is a useful tool to visualize and quantify the morphological features of teeth, which can provide the basis for a better understanding of tooth evolution linking morphology and development.

KEY WORDS: Molar, Enamel–dentine junction, Odontometry, Geometric morphometrics, Inhibitory cascade model

Introduction

Most mammalian teeth vary in shape and can be grouped into three families: incisiform, caniniform, and molariform. Morphological similarity within each tooth type was originally interpreted as the product of merism or the repetition of segments (Bateson, 1894). Dental rows of each tooth type, however, exhibit notable shape differences rather than repetition of identical elements. The differences in serially repeated morphology within an organism is called metameric variation and is thought to be a result of slight alterations in the developmental process (Weiss, 1990). Morphological variation within a tooth row is a type of metameric variation.

In humans, the metameric variation can be best assessed by investigating molars because they are the only tooth type with three elements. The human maxilla contains three sets of molars: upper first, second, and third molars (UM1, UM2, and UM3, respectively). UM1 is considered to be more stable than UM2 and UM3 with regard to development and evolution, while the distal UM3 is considered to be the most variable (Garn et al. 1963; Sofaer et al. 1971; Townsend et al. 2003; Harris & Dinh, 2006). Various studies have shown the hierarchical structure of the teeth is determined by processes of dentition patterning (*e.g.*, Butler, 1939; Dahlberg, 1945; Osborn, 1978) during orofacial development. Two hypothetical models have been proposed to explain how the differences in stability and variability between molars are determined during development (Nanci, 2013). The first is the field theory which postulates that the mesial-distal gradient of diffusible signaling molecules, so called morphogens, determines the specific fields of each tooth type (Butler, 1939). According to Butler's theory, each field contains a "key tooth" at the most mesial position which shows greater stability in size and morphology than the other teeth in the same field. Following this model, the tooth located closest to the key tooth exhibits smaller variation than more distal teeth because their tooth germs are controlled more strictly by morphogens than those located further away. In contrast, the second theory, known as the clone theory (Osborn, 1978), postulates that each tooth type is stand alone in terms of development. According to Osborn's theory, each tooth type has a single clone of preprogrammed cells located in the key tooth region that replicates with decreasing efficiency in subsequently developing teeth. Following this model, the distal teeth exhibit greater variation because their shapes are predetermined to a lesser degree than the mesial tooth.

The field and clone theories first appeared as contrasting concepts. Accumulation of experimental data, however, indicates they actually complement each other (Mistiadis & Smith, 2006). Kavanagh et al.'s experimental study (2007) synthesized the field and clone theories in a most fundamental way to form the inhibitory cascade model. Kavanagh et al. (2007) showed tooth morphology is not controlled by different concentrations of diffusible signaling molecules; instead, the activator–inhibitor dynamics determines the size differences between molars. The development of each molar is controlled by the balance between inhibitor molecules from mesially-located tooth germs and activator molecules from the mesenchyme. The ratio of genetic activation and inhibition during development determines the relative size of the teeth in the molar row. The inhibitory cascade model is linked to the field and clone theories in the following respects. The inhibitory cascade model predicts that the development of the first molar (M1) dominates the size variations of M2 and M3. This is analogous to the concept of key tooth in the field theory. On the other hand, the inhibitory cascade model posits that isolated tooth germs can continue to grow and initiate sequential tooth development, as predicted by the clone theory. Morphological variations of the molar row can thus be explained better by the inhibitory cascade model instead of the field or clone theories alone.

Such activator–inhibitor signaling mechanism is reiteratively used at a local level for cusp formation within a tooth crown (Jernvall & Thesleff, 2000, 2012; Salazar-Ciudad, 2012). In the individual tooth crown, the number and spatial patterning of cusps are determined by the iterative activation of secondary enamel knots and by the same reciprocal signaling cascade within and between the oral epithelium and mesenchyme (patterning cascade model; Jernvall & Jung, 2000; Jernvall, 2000). The activator–inhibitor signaling mechanism is thus used in the developmental processes of molars recursively, that is, at a higher level for size determination and at a more local level for cusp formation (as explained by inhibitory cascade model and patterning cascade model, respectively). Due to the reiterative nature of tooth development, the perturbations in later cascade events are amplified by those during earlier cascade events. The developmental cascades result in the hierarchical structure of the tooth morphology. In other words, the morphology of each molar and the metamerism variation as a whole contain relevant information that could help understand the developmental processes. Thus, studying metamerism variation is of special relevance for examining the relationship between

odontogenetic models and tooth morphology.

Developmental mechanisms of the tooth are increasingly invoked to interpret morphological variations in addressing phylogenetic and taxonomic issues in humans, and their living and fossil relatives of apes (hominoids) under the condition that the dental traits are independent of each other (Pilbrow, 2007; Suwa et al. 2007, 2009; Skinner et al. 2008, 2009a, b; Gómez-Robles et al. 2012, 2015). It has recently been pointed out, however, that most of the dental traits are dependent on each other, and those used to infer the phylogenetic relationships can be developmentally correlated with each other (Kangas et al. 2004). While hypothetical models are now linked to molecular signaling pathways and developmental genetics, the association between macro-level morphologies and developmental processes remains largely unexplored. The most straightforward method to do this would be experimental verification, but it is difficult in living humans and impossible in fossil species to manipulate the developmental programs and/or track the developmental processes. One possible solution is to identify metameric variation because it serves as a key for linking the morphology to the development (Weiss, 1990; Hlusko, 2002; Braga et al. 2010; Singleton et al. 2011). Furthermore, they could also be used to infer ecological and functional adaptations (Kavanagh et al. 2007; Polly, 2007).

Metameric variation in dentition remains relatively unexplored owing to difficulty in quantifying the complex shape variation in molar crowns. Some characteristic dental traits such as Carabelli's trait have been analyzed qualitatively using morphological scoring procedures (Turner et al. 1991). However, these methods only analyze specific characteristics, and do not permit demonstration of the morphological features of the entire crown or covariations among them. Other studies used quantitative data such as crown and cusp diameters to appraise morphological differences between them. Conventional quantitative methods are, however, not adequate for evaluation of the complicated morphology of dental crowns (Rizk et al. 2013). Recently, new morphometric methods [*e.g.*, geometric morphometrics (GM)] combined with micro-CT (μ CT) data have enabled more detailed quantification of tooth morphology (*e.g.*, Skinner et al. 2009a; Braga et al. 2010; Singleton et al. 2011; Morita et al. 2014a). Most of these techniques assume homology of dental features among all specimens in the analysis. For example, GM requires homology among anatomical points of reference (so-called landmarks). However, molars used in the analysis do not always share homology (*e.g.*, the absence of

hypocone), which limits the application of these techniques to the analysis of metamer variation. For example, GM does not permit analysis of UM1, UM2, and UM3 together. Because the morphology of human maxillary molars is highly variable (Fig. 1), it is difficult to establish point-to-point homology between molar specimens. It is sometimes difficult to identify homology even within the same molar in conspecific individuals (Fig. 1). Other solutions include a landmark-free approach such as morphometric mapping (MM) (Zollikofer & Ponce de León, 2001; Bondioli et al. 2010; Morimoto et al. 2011, 2012, 2014), two-dimensional (2D) surface-based approach (Boyer et al. 2011), and spherical harmonics (Specht et al. 2007; Shen et al. 2009). Here, we apply MM to human molars to analyze metamer variation. Methods of MM have been previously used to assess morphologies of long bones and dental roots (Zollikofer & Ponce de León, 2001; Bondioli et al. 2010; Morimoto et al. 2011, 2012, 2014), and have reported great merit in dense sampling data of three-dimensional (3D) morphology without the need for pre-defined anatomical structures. Furthermore, it facilitates the visual inspection and exploration of morphometric data by demonstrating detailed morphological features of 3D objects as 2D images. MM-based analysis thus permits quantification of the complex morphology of molars and analysis of metamer variation among molars without assuming homology for morphometric data acquisition and analysis.

This paper has two main aims. The first is to apply MM to quantify and visualize metamer variation among human maxillary molars and the second aim is to clarify whether there is any difference between molar crowns in phenotypic variation and variability. Variation is defined as the observed phenotypic differences, whereas variability is defined as the tendency or potential of an organism to vary (Wagner & Altenberg, 1996). Phenotypic variability corresponds to the potential range or distribution of morphological variation which reflects developmental processes and their interactions (Hallgrímsson et al. 2002; Willmore et al. 2007). Exploring phenotypic variation and variability among molars allows us to elucidate whether morphogenetic models of molar rows (inhibitory cascade model) and molar crowns (patterning cascade model) are adaptable to human maxillary molars.

Materials and Methods

A total of 176 specimens (UM1: $N = 62$, UM2: $N = 54$, UM3: $N = 60$) were used in this study (Table 1). Sex was unknown for most of the sample cohort which was a mixture of populations from different periods and regions (from Jomon, medieval, early modern, and modern populations in the Japanese archipelago; see Table 1 for details). The sample structure with mixed populations does not violate the aim of this study to investigate patterns of metameric variation in human molars because potential variation due to differences in periods and/or regions are minimal compared with between molar differences (Kondo & Yamada, 2003; Morita et al. 2014). Right and left teeth were pooled to maximize sample size. Teeth that had completed crown formation and maintained unworn enamel–dentine junction (EDJ) were used. To perform μ CT scanning, isolated teeth were collected, and only a single tooth in the molar row from each individual was available as isolated teeth in the present sample. The μ CT images of right molars were transformed into mirror images using the software package ImageJ (NIH, USA), and all specimens were regarded as left side. EDJ was used to avoid adverse effects of dental wear on shape analysis. It is the boundary between the epithelial and mesenchymal components during odontogenesis that possesses information regarding the original crown shape (Kraus & Jordan, 1965) and is significantly correlated with the shape of the outer enamel surface of teeth (Skinner et al. 2009; Morita et al. 2014b). Most of the UM1 specimens were scanned using a μ CT scanner (ScanXmateA080S, Comscantecno, Japan; housed at Kyoto University) with the following data acquisition and image reconstruction parameters: 80 kV, 125 μ A, voxel resolution of 31–32 μ m. The remaining specimens were scanned using a μ CT scanner (ELE SCAN, Nittetsu Elex, Japan; housed at Niigata University) with the following parameters: 80kV, 100 μ A, voxel resolution of 30 μ m. To facilitate tissue segmentation, the image stack for each tooth was filtered with a median filter, and triangular mesh models of EDJ were reconstructed three dimensionally using the 3D viewer plug-in in ImageJ.

To generate the least-squares plane as an approximation of the cervical plane, the cervical line of each tooth was manually digitized (50–60 points depending on the size of each tooth) using MeshLab 1.3.3 software. This plane was used to determine the baseline of EDJ crown (Fig. 2A). The tooth was then aligned such that the least-squares plane was in accordance with the xy -plane of the

Cartesian coordinate system, where its origin was defined by the centroid of the cervical line (Fig. 2A). In the coordinate system, the following three morphometric variables were sampled; surface curvature, height, and radius. The mean curvature of EDJ surface (c) was calculated analytically for each vertex of the 3D model (Appendix A; note the surface curvature is not calculated along a cross-sectional outline; instead it is calculated on the surface and the resulting curvature value is sampled along the outline. See below). The resulting positive and negative values of c indicate the convex and concave EDJ surfaces, respectively. The height from the cervical plane (h) and the radius from the centroid of the cervical line (r) were calculated directly from the 3D coordinates of the surface mesh (Fig. 2).

For each specimen, the three variables (c , h , and r) were sampled from each cross-sectional outline and around the entire EDJ surface. EDJ surface was digitally sectioned equiangularly ($L = 300$) by a plane orthogonal to the xy -plane and through the centroid. In each cross section, the outline that runs from the point located just above the centroid of the cervix to the point at the level of the xy -plane was parameterized with elliptic Fourier analysis (EFA) equidistantly ($K = 300$) (Fig. 2B). EFA was used to reduce noise and to define parametric outline functions (Kuhl & Giardina, 1982). They were mapped onto a polar coordinate system (d, θ), where d denoted the normalized position along each cross-sectional outline ($d = 0 \rightarrow 1$: centroid \rightarrow cervix) and θ denoted the anatomical direction [$\theta = 0^\circ \rightarrow 360^\circ$: buccal (0°) \rightarrow mesial (90°) \rightarrow lingual (180°) \rightarrow distal (270°) \rightarrow buccal (360°): Figs. 2C, D, E, and F]. EDJ could be visualized using 2D morphometric maps $M(d, \theta)$, and the distributions, $c(d, \theta)$, $h(d, \theta)$, and $r(d, \theta)$, could be represented as $K \times L$ matrices, respectively, where K and L denoted the number of elements along d and θ , respectively ($K = L = 300$).

The effects of scaling were corrected as follows in our analysis. The variables h and r were calculated from the 3D mesh that was normalized by centroid size (the square root of the summed squared distances of $K \times L$ 3D coordinates) (Bookstein, 1991). This is analogous to the ordinary geometric morphometric method. With regard to the variable c , we sampled the data of each tooth, constructed the matrix that represented c -M, and then normalized the data using the z-score of each c -M. Each row of the $K \times L$ matrix for each specimen was sequentially weighted by a concentrically subdivided area with radius 1 and constant internal angle ($= 1/L$) that was equidistantly sectioned ($= 1/K$) (Appendix B).

For the comparative analysis of the morphometric maps M_i of all specimens ($i = 1, 2, \dots, N$), differences between specimens in orientation around the centroid (θ) had to be minimized. First, all specimens were pre-aligned manually to orientate them in a similar anatomical direction (Fig. 2C). Thereafter, optimal fitting was performed by iteratively minimizing the inter-specimen distance in Fourier space through rotation around θ [vertical (occlusal-cervical) axis; z -axis (Fig. 2A)], and this was executed by calculating a consensus map (using pre-aligned MMs for the first time) and aligning each MM to this consensus. This procedure was repeated until differences between specimens were minimized. The 2D-Fourier transforms $F(M_i)$ of all M_i were then calculated (M has natural periodicity in θ) so as to produce $K \times L$ sets of Fourier coefficients that represent the shape of EDJ surface of each specimen as a point in the multidimensional Fourier space. The Fourier transform (FT) represents MMs as a set of spatial frequencies with associated amplitudes. A basic property of the FT is the low-frequency domain captures global features (*i.e.*, large-scale variation), while the high frequency domain captures local features (*i.e.*, small-scale variation). Low-pass filtering in Fourier space (*i.e.*, removal of the high-frequency domain as noise) thus allows us to capture variation in global features. The most relevant statistical information about shape variation in the sample is typically contained in the low frequency domain (Zollikofer & Ponce de León, 2005). Using low-pass filtering in Fourier space, principal components analysis (PCA) was performed to identify principal patterns of shape variation in the sample. To facilitate visual inspection and morphological interpretation of the results of PCA, morphometric maps were reconstructed by transforming an arbitrary point in PC space into its corresponding sets of Fourier coefficients and then applying an inverse transformation. Morphometric maps were visualized using a false-color mapping scheme. We also performed landmark-based GM methods to compare the new methods of MM proposed here with earlier methods (Appendix C).

Allometric scaling patterns among molars were explored by calculating a multivariate regression of shape PCs vs. log centroid size (Penin et al. 2002; Zollikofer & Ponce de León, 2006). This approach permits comparison of tooth morphology changes with size differences (allometric patterns) in multivariate shape space (morphospace). Bootstrapping was used to test the differences in mean shape between maxillary molars, and the tooth-specific distribution patterns in morphospace that were calculated as the distance between tooth-specific variance-covariance matrices (Mitteroecker &

243 Bookstein, 2009). Shape variation was measured by calculating the square root of the sum of the
244 squared distances between mean configuration and each specimen in morphospace (Polly, 1998;
245 Jernvall, 2000). To test whether there was a significant difference in shape variation among molars, a
246 nonparametric Kruskal-Wallis test was performed, followed by multiple comparisons corrected by the
247 Bonferroni method (Rice, 1989). All calculations were performed by W.M. and N.M. using the
248 software package MATLAB 8.1, MathWorks, USA (codes are available on request).

Results

Fig. 2 shows a visual comparison of the 3D representation of EDJ morphology and its corresponding MMs for UM1. EDJ surface and MMs show marked features that were associated with the characteristics of the enamel surface. Hence, we used anatomical terms for the enamel surface to indicate EDJ features (see Fig. 2). MM of surface curvature (c -M) (Fig. 2D) captured well-defined anatomical features; four cusps (paracone, protocone, metacone, and hypocone), Carabelli trait, ridges that are located between the cusps and delimit the occlusal table, the oblique crest, buccal and lingual grooves, and trigon and talon basins (mesially and distally located depressions, respectively). MM of height (h -M) from the cervix (Fig. 2E) captured relative location and distribution of the cusps. MM of radius (r -M) from the centroid of the cervical line (Fig. 2F) gave a comprehensive view of the horizontal dimensions of EDJ. For example, the difference in outward inclination is indicated by the difference in color gradation (more vertical on medial and distal sides vs. more inclined on buccal and lingual sides).

The MM-based shape variation of the entire sample was explored using PCA for all morphometric variables. PC scores of MM-based and conventional GM analyses were compared and found to be similar to each other (Appendix C). We visualized the shape variation along the direction in morphospace that distinguished the average shapes of UM1, UM2, and UM3 (see *e.g.*, Lordkipanidze et al. 2013, used a similar approach) in order to explore the shape variation independent of sample structure. For the purpose of easier visual inspection and interpretation of data plotting, we rotated PC1 and PC2 so as to maximize the within-versus between-molar variation, and obtained a set of shape components SC1 and SC2, as shown in Fig. 3 (original PC1 and PC2 plot is shown in Fig. S1). SC1 and SC2 thus distinguish between UM1 and UM2/UM3, and UM1/UM2 and UM3, respectively. The results showed that morphological variation between maxillary molars along mesio-distal direction was not represented linearly in the morphospace; instead, lines connecting average shapes of UM1–UM2 and UM2–UM3 are almost perpendicular to each other (Fig. 3).

Extreme shapes along each SC axis are shown in Fig. 3. Features shown by positive SC1 in each MM are summarized as follows: c -M, pointed tip of each of the four cusps, larger relief in the occlusal table and lingual surface, and relatively larger talon against trigon separated by oblique crest;

h-M, relatively higher cusps; and *r*-M, larger dimension in each of the four cusp directions, particularly toward paracone. On the other hand, negative SC1 exhibited the following features: *c*-M, development of marginal ridges and tendency of hypocone reduction; *h*-M, relatively lower cusps, disappearance of hypocone, and protocone and metacone are located more disto-lingually; and *r*-M, larger bucco-lingual dimension in the mesial cusps. Collectively, SC1 exhibited shape variation associated with hypocone development and reduction. Features observed at the positive extreme of SC2 were as follows: *c*-M, blunt cusp tips and decreased relief in the occlusal table; *h*-M, generally lower cusps and rounded outline of the occlusal table; and *r*-M, relatively round outline of the occlusal table. On the other hand, negative SC2 exhibited the following features: *c*-M, clear cusp tips and increased relief; *h*-M, higher cusps, more distally located protocone, and more lingually located metacone; and *r*-M, elliptical outline of the occlusal table with a long axis in the paracone-hypocone direction. Collectively, SC2 exhibited shape variation associated with different heights and shapes of the occlusal table.

Because tooth-specific distribution patterns associated with size differences were approximately linear, size-related shape changes were visualized as tooth-specific vectors in morphospace (allometric vector) (Fig. 3). In the PC plot graph, smaller and larger teeth were located around the bottom and head of the arrow, respectively (Fig. 3). The directions of the allometric vectors of UM2 and UM3 demonstrated that EDJ morphology approached shape of UM1 as the size increased. Allometric vector was also calculated and depicted for all specimens together (common allometric vector). The common allometric vector was also orientated with a direction similar to UM2- and UM3-specific allometric vectors. In contrast, the direction of the allometric vector of UM1 was distinct from UM2- and UM3-specific allometric vectors and from the common allometric vector. The larger-sized UM1 was characterized by a relatively rounded outline of the occlusal table. The shape variation along the axis perpendicular to the allometric vector indicates variation independent of allometry. In UM2, the shape variation along the allometric vector (*i.e.*, size-dependent variation) was greater than the variation independent of allometry (Fig. 3). In UM3, the shape variation along the allometric vector was comparable to the variation independent of allometry. In UM1, on the other hand, the shape variation due to allometry was comparable to the variation independent of allometry. Thus, allometry explained, to a large extent, the shape variation in UM2 and UM3, and to a lesser extent that

305 in UM1.

306 MM-based shape distances among molars were significant for all molar-shape comparisons
307 (Table 2). UM1 showed greater shape disparity from UM2 ($D = 1.97$), and UM3 ($D = 2.30$) than that
308 between UM2 and UM3 ($D = 1.71$). Fig. 4 shows MM-based representations of the average shapes of
309 each molar. The mean shape of UM1 is characterized by four well-defined cusps that are developed in
310 the cervical and horizontal (parallel to occlusal plane) directions, and demonstrate greater surface relief
311 within the occlusal table associated with developed oblique ridge, accessory ridges, and inter-cusp
312 grooves. The average UM2 shape is characterized by developed inter-cusp marginal ridges, but the
313 relief located inside the occlusal table is relatively obscure and the hypocone shows a slight reduction.
314 UM3 is characterized by rounded inter-cusp outline ridge, decreased and mesially-biased relief, overall
315 reduction of cusp formation, and remarkable hypocone reduction. The tests of group-specific modes of
316 variation (distances between variance-covariance matrices) yielded a significant result only for the
317 comparison between UM1 and UM3 (Table 2). The size of phenotypic variation showed that UM3 was
318 significantly more variable than both UM1 and UM2 (Fig. 5).

Discussion

Metameric variation in terms of shape variation, variability, and allometric effects was assessed using methods of MM. Our data showed that metameric variation in human maxillary molars was not represented as a simple morphological gradation. UM1, UM2, and UM3 exhibited considerable tooth-specific shape variation, and morphological changes from UM1 to UM2 and from UM2 to UM3 differed from each other.

UM3 showed unique variability compared with UM1 and UM2 in two respects. First, it exhibited the largest morphological variation (Fig. 5), and this was consistent with previous studies that reported large variation of UM3 using conventional quantitative methods (Garn et al. 1963; Sofaer et al. 1971; Townsend et al. 2003; Harris & Dinh, 2006). Second, UM3 showed a distinct distribution pattern (*i.e.*, distinct shape of the point cloud) in morphospace (Table 2). The unique pattern of variability of UM3 could be explained by the physical and developmental constraints. With regard to physical constraint, the amount of available space in a jaw can affect the UM3 variability because it is the last tooth to form in a dentition, whereas developmental constraints include the underlying stochastic nature of sequential molar formation which can contribute to greater shape variation (Townsend et al. 2003). Specifically, larger variation of UM3 can be interpreted as a consequence of developmental processes described by the inhibitory cascade model (Kavanagh et al. 2007), which suggests that the developmental processes of a molar row may produce cumulative effects of local epigenetic events, particularly on the UM3 which forms last.

Analyses of allometry showed a considerable portion of the shape variation of UM2 can be explained by size variation, and EDJ morphologies of UM2 and UM3 resemble the shape of UM1 with increasing size (Fig. 3). The common allometric vector of the entire sample also showed a tendency to resemble the patterns of UM2 (Fig. 3). This indicates the morphology of human maxillary molars has a tendency to converge toward the morphology of UM1, which can therefore play an important role in determining the morphologies of UM2. Taking into account the development of M1 affects the sizes of M2 and M3 (Kavanagh et al. 2007), our data indicated that human maxillary molars are not pre-programed to realize distinct morphologies, but are morphologically integrated as a whole by the development of “key” UM1 which controls the sizes of UM2 and UM3 (Braga and Heuzé, 2007). The

morphometric data presented in this study could thus give support to the hypothetical notion that UM1 is a “key tooth” (Butler, 1939; Dahlberg, 1945). It should be noted, however, that our data also indicate the “rule” of key tooth theory is not easily generalized. While UM3 in general shows a similar pattern of allometry with UM2, the allometric pattern of UM3 differs from that of UM2 in two respects. First, size-independent variation (i.e., variation along the direction perpendicular to the allometric vector) is considerably large relative to size-related variation (i.e., variation along the allometric vector) in UM3 compared to UM2. Second, the allometric vector of UM3 is directed toward large-sized UM1 while allometric vector of UM2 is directed fairly toward the mean shape of UM1. Thus, it remains elusive how and why the tooth-specific allometric patterns differ from each other, and how the actual pattern of molar morphology deviates from the “rule” of key tooth theory.

UM1 showed a different allometric pattern from UM2 and UM3 (Fig. 3). As the size of EDJ increased, the outline of the occlusal table became circular in UM1. This may be related to an increase in the individual cusp size associated with increases in entire EDJ size because increase in the individual cusp size can result in relatively equal proportion of each cusp size. In this context, the circular outline in UM1 is distinct from that of the occlusal table observed in UM3.

Our data showed UM1 exhibited smaller variation of size than UM2 and UM3 (Table S2) as previously reported (Garn et al. 1963). This seems to be contradictory because the sizes of distal molars are constrained by mesial molars according to the inhibitory cascade model. The larger variation of UM2 and UM3 observed in this study, however, suggests they are not constrained in terms of phenotypes but are constrained in terms of the independence of developmental pathways reflecting the downstream position of stochastic cascade events. On the other hand, smaller size variation of UM1 indicates it exhibits the most stable and inherent odontogenetic potential among molar teeth. It is thus sensible to note our data are indeed in accordance with, rather than contradictory to, the inhibitory cascade model.

Morphological differences between molars were evaluated as distances in morphospace. The results show that the phenotypic distances between UM1 and UM2 and between UM1 and UM3 are larger than the distance between UM2 and UM3 (Table 2). This indicates UM1 is phenotypically distinct among the maxillary molars. The distinct morphology and allometric pattern of UM1 and the

unique variability of UM3 may reflect, in part, the timing of tooth formation [during embryonic period (UM1) vs. after birth (UM3)]. Moreover, the period up to completion of tooth formation is considerably shorter in UM1 than in UM2 and UM3 (Schour & Massler, 1941). Thus, we speculated that temporal differences in onset and/or termination of tooth formation could be associated with between-taxon differences of tooth morphology and metameric variation to some extent in hominoids.

The *r*-Ms captured a stable pattern which we may call “paracone protuberance”, that is, the radius from the centroid of the cervical line was the largest in the direction of paracone (represented as red in false-color map) (Figs. 2F, 3, and 4). This tendency is relatively stable and is independent of molar position and allometric effects. After excluding the effects of allometry and tooth position, it is likely that these observations reflect genetically determined developmental processes. It is probable that the pattern of the general shape of molars is constrained by the sequence of cusp formation which is initiated in the order from mesial to distal (paracone→protocone→metacone→hypocone) (Turner, 1963; Kraus & Jordan, 1965). It is sensible that the area around the first-forming cusp would be larger in the mesio-buccal direction, regardless of surface curvature and cusp height.

The *c*-M captured a pattern in the surface relief which we may call “mesio-distal topographical gradient”, that is, the more distal the teeth are located, the more marked is the contrast of surface topography between mesio-buccal vs. disto-lingual sides (Figs. 3, 4). For example, in UM2 and UM3, the paracone-protocone ridge is well developed compared with the metacone-hypocone ridge, and the trigon basin exhibits deeper depression than the talon basin (Fig. 4; *c* and *r*-M). Moreover, in UM2 and particularly in UM3, the distal cusps (metacone and hypocone) are degenerated compared with the mesial cusps (paracone and protocone) (Fig. 4; *c* and *r*-M). The mesio-distal gradient of the surface topography has been reported in previous studies that focused on metameric variation among human maxillary molars (Yamada & Brown, 1988, 1990; Macho & Moggi-Cecchi, 1992; Kondo & Yamada, 2003; Kondo et al. 2005; Kondo & Townsend, 2006). The dentine horns and ridges on EDJ correspond to the cusp tips and ridges on the enamel surface, and are formed by the folding of the inner-enamel epithelium in response to the formation of secondary enamel knots (Jernvall & Jung, 2000). Tooth morphology is controlled by the combined effects of biochemical signaling degraded from mesial to distal direction at the tooth row level and at the individual crown level (Weiss, 1990; Jernvall

& Thesleff, 2000; Harris & Dihn, 2006). It is likely that the genotypic potential is expressed to its full extent phenotypically only when the effect of the morphogenetic signaling is extended sufficiently during odontogenesis (Kondo & Townsend, 2006). As a consequence, all of the primary enamel knots and resulting surface topography are well formed in the development of UM1, while the distal primary enamel knots and resulting surface topography are degenerated compared with the mesial primary enamel knots in the development of distal teeth. The mesio-distal gradient of the surface topography can thus be reasonably linked to the mesio-distal gradient of biochemical signaling.

The patterning cascade model proposed a formation sequence of “mesial first” and “distal later” as the principle of dental patterning (Jernvall, 2000). Taking into account the “paracone protuberance” in general shape, and “mesio-distal topographical gradient” in surface relief together, the phenotypic patterns observed in this study can in general be interpreted to be in accordance with the patterning cascade model. Furthermore, the nested hierarchical structure of reciprocal signaling interaction (Jernvall & Thesleff, 2000, 2012) can result in a mesio-distal morphological gradient at the inter-molar level (macro-patterning) and at the inter-cusp level (micro-patterning), shown by the experimental data (Cai et al. 2007).

We interpreted observed patterns of morphological variation and variability in terms of tooth development, but various issues remain to be addressed to further our understanding of the link between developmental processes and phenotypes. For example, only a single tooth was obtained from each individual in this study. To assess effects of environmental and/or epigenetic factors more specifically, sampling teeth from the same individuals would be worthwhile to corroborate the results presented in this study. The present sample consists of populations from different periods and regions. It would also be interesting to compare between-population variation in time and space in future studies.

A comparison of landmark-based and MM-based methods showed that both methods are equally efficient in detecting patterns of morphological variation and variability. Thus, semilandmark-based methods, especially combined with surface-based visualization (Gunz et al. 2005), can be potentially used for analyzing metameric variation of tooth if point-to-point homology between specimens can be established. On the other hand, MM-based approach does not require *a priori* definition of landmarks (e.g., cusps, ridges and depressions). Our results showed that MM-based

methods can be applied to molars of which the homology between individuals is extremely difficult (Fig. 1). This study also showed that MM-based methods are suitable tool for visual inspection of anatomical features of molars (Figs. 2, 3, 4). Between- and within-molar variation of anatomical features were effectively analyzed based on quantitative data using the methods presented in this study.

Using three morphometric parameters (*c*: surface curvature, *h*: height, and *r*: radius), we quantified EDJ morphology by means of the MM methods. Our results indicate the data expressed by each morphometric variable can be interpreted in the framework of development. The *h* and *r*-Ms allow clear visualization of global morphological features, such as the presence/absence of cusps. They also allow expression of global EDJ morphology that could reflect the epithelial elongation toward the cervical loop, the ratio and period of tooth development, and/or the available space for tooth germ growth (Jernvall, 1995; Salazar-Ciudad, 2012). While the *h* and *r*-Ms on EDJ surface are representative of tooth germ growth, the subsequent enamel formation process can also be quantified by the application of MM methods to enamel thickness. The *c*-M permits capture and analysis of subtle surface topographies that are conventionally recognized as nonmetric dental traits. The topological characters shown in *c*-M result from the epithelial undulation regulated by the mesenchyme and by the mechanical interaction on the basement membrane during morphogenesis (Jernvall & Jung, 2000; Salazar-Ciudad, 2008). For example, a clear representation of Carabelli's trait may be related to the expression of an additional secondary enamel knot (Fig. 2D). To this end, further experimental analyses, whether *in silico* experiments (*e.g.*, Salazar-Ciudad & Jernvall, 2010) with hominoids or *in vitro/in vivo* experiments with model animals (*e.g.*, Harjunmaa et al. 2012, 2014), are required to link the surface curvature to expression patterns of signaling molecules.

Using dental traits presents some difficulties for the reconstruction of phylogeny because it is likely that the morphological characters in molars are not independent from each other but are developmentally correlated (Kangas et al. 2004). Our results indicate capturing taxon-specific dental features such as metamerism variation can be a useful complement because they encapsulate taxon-specific patterns of tooth development. This study showed MM is a useful tool for exploring metamerism variation and linking the tooth morphology to development. Thus, using it as an exploratory tool of tooth morphology has great potential for a better understanding of evolution of teeth in terms of

459 morphological, developmental, functional, and adaptive aspects.

Conclusion

We applied MM to EDJ of human maxillary molars. Our results showed that MM is a useful tool to explore morphological variation of teeth. We also found that UM1 is phenotypically distinct among the maxillary molars and is characterized by four well-defined cusps and greater surface relief within the occlusal table. On the other hand, UM3 is characterized by decreased surface relief and rounded within the occlusal table and it also exhibits a unique variability pattern with greater shape variation and a distinct distribution pattern in morphospace. The UM2 represents an intermediate state between UM1 and UM3 in terms of phenotypic variation and variability. Tooth-specific patterns of allometry indicated that the morphology of the human maxillary molar tends to converge toward that of UM1. These results are generally in accordance with morphogenetic models of molar rows (inhibitory cascade model) and molar crowns (patterning cascade model). Our data thus show that morphological variation of human molars can be explained to a great extent by the framework of development.

472 **Acknowledgments**

473 The authors thank T. Domon, S. Takahashi, H. Ida-Yonemochi, and K. Saito for thoughtful
474 discussion and comments. We are grateful to M. Nakatsukasa, K. Hirata, T. Nagaoka, M. Abe, K.
475 Shimatani, and K. Miyazawa for access to specimens. We are also grateful to three anonymous
476 reviewers for their useful comments and suggestions. This work was supported, in part, by JSPS
477 KAKENHI Grant no.25293371 to H.O., no.11J00940 to W.M., and no.15H05609 to N.M. The authors
478 declare no potential conflicts of interest with respect to the authorship and/or publication of this article.

479 **Author Contributions**

480 W. M. contributed to study conception, design, acquisition, data analysis, interpretation, and
481 drafting and critical revision of the manuscript. N. M. contributed to design, data analysis, interpretation,
482 and drafting and critical revision of the manuscript. H. O. contributed to study conception, design,
483 interpretation, and drafting and critical revision of the manuscript. All authors gave final approval and
484 agree to be accountable for all aspects of the work.

References

- Bateson W (1894) *Materials for the Study of Variation: Treated with Special Regard to Discontinuity in the Origin of Species*. London: Macmillan.
- Bondioli L, Bayle P, Dean C, et al. (2010) Technical note: Morphometric maps of long bone shafts and dental roots for imaging topographic thickness variation. *Am J Phys Anthropol* 142, 328–334.
- Bookstein FL (1997) *Morphometric Tools for Landmark Data: Geometry and Biology*. Cambridge: Cambridge University Press.
- Boyer DM, Lipman Y, Clair ES, et al. (2011) Algorithms to automatically quantify the geometric similarity of anatomical surfaces. *Proc Nat Acad Sci USA* 108, 18221–18226.
- Braga J, Heuzé Y (2007) Quantifying variation in human dental developmental sequences: An EVO-DEVO perspective. In: *Dental Perspectives on Human Evolution: State of the Art Research in Dental Anthropology*. (eds Bailey SE, Hublin JJ), pp. 247–261. Dordrecht: Springer Netherlands.
- Braga J, Thackeray JF, Subsol G, et al. (2010) The enamel–dentine junction in the postcanine dentition of *Australopithecus africanus*: Intra-individual metamerism and antimeric variation. *J Anat* 216, 62–79.
- Butler PM (1939) Studies of the mammalian dentition-differentiation of the post-canine dentition. *Proc Zool Soc Lond B* 109, 1–36.
- Cai J, Cho SW, Kim JY, et al. (2007) Patterning the size and number of tooth and its cusps. *Dev Biol* 304, 499–507.
- Dahlberg AA (1945) The changing dentition of man. *J Am Dent Assoc* 32, 676–690.
- Garn SM, Lewis AB, Kerewsky RS (1963) Third molar agenesis and size reduction of the remaining teeth. *Nature* 200, 488–489.
- Gómez-Robles A, de Castro JMB, Martín-Torres M, Prado-Simón L, Arsuaga, JL (2012). A geometric morphometric analysis of hominin upper second and third molars, with particular emphasis on European Pleistocene populations. *J Hum Evol* 63, 512–526.
- Gómez-Robles A, de Castro JMB, Martín-Torres M, Prado-Simón L, Arsuaga, JL (2015) A geometric morphometric analysis of hominin lower molars: Evolutionary implications and

- 513 overview of postcanine dental variation. *J Hum Evol* 82, 34–50.
- 514 Gunz P, Mitteroecker P, Bookstein FL (2005). Semilandmarks in three dimensions. In: *Modern*
515 *Morphometrics in Physical Anthropology*. (ed Slice DE), pp. 73–98. New York: Springer.
- 516 Hallgrímsson B, Willmore K, Hall BK (2002) Canalization, developmental stability, and morphological
517 integration in primate limbs. *Am J Phys Anthropol* 35, 131–158.
- 518 Harjunmaa E, Kallonen A, Voutilainen M, Hämäläinen K, Mikkola ML, Jernvall J (2012) On the
519 difficulty of increasing dental complexity. *Nature* 483, 324–327.
- 520 Harjunmaa E, Seidel K, Häkkinen T, et al. (2014) Replaying evolutionary transitions from the dental
521 fossil record. *Nature* 512, 44–48.
- 522 Harris EF, Dinh DP (2006) Intercusp relationships of the permanent maxillary first and second molars
523 in American whites. *Am J Phys Anthropol* 130, 514–528.
- 524 Hlusko LJ (2002) Identifying metamerism variation in extant hominoid and fossil hominid mandibular
525 molars. *Am J Phys Anthropol* 118, 86–97.
- 526 Jernvall J (1995) Mammalian molar cusp patterns: Developmental mechanisms of diversity. *Acta Zool*
527 *Fennica* 198, 1–61.
- 528 Jernvall J (2000) Linking development with generation of novelty in mammalian teeth. *Proc Nat Acad*
529 *Sci USA* 97, 2641–2645.
- 530 Jernvall J, Jung HS (2000) Genotype, phenotype, and developmental biology of molar tooth characters.
531 *Yrbk Phys Anthropol* 43, 171–190.
- 532 Jernvall J, Thesleff I (2000) Reiterative signaling and patterning during mammalian tooth
533 morphogenesis. *Mech Develop* 92, 19–29.
- 534 Jernvall J, Thesleff I (2012) Tooth shape formation and tooth renewal: evolving with the same signals.
535 *Development* 139, 3487–3497.
- 536 Kangas AT, Evans AR, Thesleff I, Jernvall J (2004) Nonindependence of mammalian dental characters.
537 *Nature* 432, 211–214.
- 538 Kavanagh K, Evans A, Jernvall J (2007) Predicting evolutionary patterns of mammalian teeth from
539 development. *Nature* 499, 427–432.
- 540 Kondo S, Yamada H (2003) Cusp size variability of the maxillary molariform teeth. *Anthropol Sci* 111,

- 541 255–263.
- 542 Kondo S, Townsend GC, Yamada H (2005) Sexual dimorphism of cusp dimensions in human
543 maxillary molars. *Am J Phys Anthropol* 128, 870–877.
- 544 Kondo S, Townsend GC (2006) Associations between Carabelli trait and cusp areas in human
545 permanent maxillary first molars. *Am J Phys Anthropol* 129, 196–203.
- 546 Kraus BS, Jordan RE (1965) *The human dentition before birth*. Philadelphia (PA): Lea and Febiger.
- 547 Kuhl F, Giardina C (1982) Elliptic Fourier features of a closed contour. *Computer graphics and image*
548 *processing* 18, 236–258.
- 549 Lordkipanidze D, de León MSP, Margvelashvili A, et al. (2013) A complete skull from Dmanisi,
550 Georgia, and the evolutionary biology of early *Homo*. *Science* 342, 326–331.
- 551 Macho GA, Moggi-Cecchi J (1992) Reduction of maxillary molars in *Homo sapiens sapiens*: a
552 different perspective. *Am J Phys Anthropol* 87, 151–159.
- 553 Mitsiadis TA, Smith MM (2006) How do genes make teeth to order through development? *J Exp Zool*
554 *B Mol Dev Evol* 306, 177–182.
- 555 Mitteroecker P, Bookstein F (2009) The ontogenetic trajectory of the phenotypic covariance matrix,
556 with examples from craniofacial shape in rats and humans. *Evolution* 63, 727–737.
- 557 Morimoto N, Zollikofer CPE, Ponce de León MS (2011) Exploring femoral diaphyseal shape variation
558 in wild and captive chimpanzees by means of morphometric mapping: a test of Wolff's Law. *Anat*
559 *Rec* 294, 589–609.
- 560 Morimoto N, Zollikofer CPE, Ponce de León MS (2012) Shared human–chimpanzee pattern of
561 perinatal femoral shaft morphology and its implications for the evolution of hominin locomotor
562 adaptations. *PLoS ONE* 7, e41980.
- 563 Morimoto N, Ponce de León MS, Zollikofer CPE (2014) Phenotypic variation in infants, not adults,
564 reflects genotypic variation among chimpanzees and bonobos. *PLoS ONE* 9, e102074.
- 565 Morita W, Yano W, Nagaoka T, Abe M, Nakatsukasa M (2014a) Size and shape variability in human
566 molars during odontogenesis. *J Dent Res* 93, 275–280.
- 567 Morita W, Yano W, Nagaoka T, et al. (2014b) Patterns of morphological variation in enamel–dentin
568 junction and outer enamel surface of human molars. *J Anat* 224, 669–680.

- 569 Nanci A (2013) *Ten Cate's Oral Histology: Development, Structure, and Function. 8th ed.* St. Louis:
570 Elsevier Health Sciences.
- 571 Osborn JW (1978) Morphogenetic gradients: field versus clones. In: *Development, Function and*
572 *Evolution of Teeth.* (eds Butler PM, Joysey KA), pp. 171–201. London: Academic Press.
- 573 Penin X, Berge C, Baylac M (2002) Ontogenetic study of the skull in modern humans and the common
574 chimpanzees: neotenic hypothesis reconsidered with a tridimensional Procrustes analysis. *Am J*
575 *Phys Anthropol* 118, 50–62.
- 576 Rice WR (1989) Analyzing tables of statistical tests. *Evolution* 43, 223–225.
- 577 Pilbrow V (2007) Patterns of molar variation in great apes and their implications for hominin taxonomy.
578 In: *Dental Perspectives on Human Evolution: State of the Art Research in Dental Anthropology.*
579 (eds Bailey SE, Hublin JJ), pp. 9–32. Dordrecht: Springer Netherlands.
- 580 Polly PD (1998) Variability, selection, and constraints: development and evolution in viverravid
581 (Carnivora, Mammalia) molar morphology. *Paleobiology* 24, 409–429.
- 582 Polly PD (2007) Development with a bite. *Nature* 449, 413–415.
- 583 Rizk OT, Grieco TM, Holmes MW, Hlusko LJ (2013) Using geometric morphometrics to study the
584 mechanisms that pattern primate dental variation. In: *Anthropological Perspectives on Tooth*
585 *Morphology.* (eds Scott GR, Irish JD), pp. 126–169. Cambridge: Cambridge University Press.
- 586 Salazar-Ciudad I (2008) Tooth morphogenesis in vivo, in vitro, and in silico. *Curr Top Dev Biol* 81,
587 341–371.
- 588 Salazar-Ciudad I (2012) Tooth patterning and evolution. *Curr Opin Genet Dev* 22, 585–592.
- 589 Salazar-Ciudad I, Jernvall J (2010) A computational model of teeth and the developmental origins of
590 morphological variation. *Nature* 464, 583–586.
- 591 Schour I, Massler M (1941) The development of the human dentition. *J Am Dent Assoc* 28, 1153–
592 1160.
- 593 Shen L, Farid H, McPeck MA (2009) Modeling three-dimensional morphological structures using
594 spherical harmonics. *Evolution* 63, 1003–1016.
- 595 Singleton M, Rosenberger AL, Robinson C, O'Neill R (2011) Allometric and metameric shape variation
596 in *Pan* mandibular molars: a digital morphometric analysis. *Anat Rec* 294, 322–334.

- 597 Skinner MM, Wood BA, Boesch C, et al. (2008) Dental trait expression at the enamel–dentine junction
598 of lower molars in extant and fossil hominoids. *J Hum Evol* 54, 173–186.
- 599 Skinner MM, Gunz P, Wood BA, Boesch C, Hublin JJ (2009a) Discrimination of extant *Pan* species
600 and subspecies using the enamel–dentine junction morphology of lower molars. *Am J Phys*
601 *Anthropol* 140, 234–243.
- 602 Skinner MM, Wood BA, Hublin JJ (2009b) Protostylid expression at the enameledentine junction and
603 enamel surface of mandibular molars of *Paranthropus robustus* and *Australopithecus africanus*. *J*
604 *Hum Evol* 56, 76–85.
- 605 Sofaer JA, Bailit HL, Maclean CJ (1971) A developmental basis for differential tooth reduction during
606 hominid evolution. *Evol Int J Org Evol* 25, 509–517.
- 607 Specht M, Lebrun R, Zollikofer CPE (2007) Visualizing shape transformation between chimpanzee and
608 human braincases. *Visual Computer* 23, 743–751.
- 609 Suwa G, Kono RT, Katoh S, Asfaw B, Beyene Y (2007) A new species of great ape from the late
610 Miocene epoch in Ethiopia. *Nature* 448, 921–924.
- 611 Suwa G, Kono RT, Simpson SW, et al. (2009) Paleobiological implications of the *Ardipithecus ramidus*
612 dentition. *Science* 326, 69–99.
- 613 Townsend G, Richards L, Hughes T (2003) Molar intercuspal dimensions: genetic input to phenotypic
614 variation. *J Dent Res* 82, 350–355.
- 615 Turner EP (1963) Crown development in human deciduous molar teeth. *Arch Oral Biol* 8, 523–550.
- 616 Turner II CG, Nichol CR, Scott GR (1991) Scoring procedures for key morphological traits of the
617 permanent dentition: the Arizona State University Dental Anthropology System. In: *Advances in*
618 *Dental Anthropology*. (eds Kelley MA, Larsen CS), pp. 13–31. New York: Wiley-Liss.
- 619 Wagner GP, Altenberg L (1996) Complex adaptations and the evolution of evolvability. *Evolution* 50,
620 967–976.
- 621 Willmore KE, Young N, Richtsmeier JT (2007) Phenotypic variability: its components, measurement
622 and underlying developmental processes. *Evol Biol* 34, 99–120.
- 623 Weiss (1990) Duplication with variation: metamerism logic in evolution from genes to morphology. *Yrbk*
624 *Phys Anthropol* 33, 1–23.

- 625 Yamada H, Brown T (1988) Contours of maxillary molars studied in Australian Aborigines. *Am J Phys*
626 *Anthropol* 76, 399–407.
- 627 Yamada H, Brown T (1990) Shape components of the maxillary molars in Australian Aborigines. *Am*
628 *J Phys Anthropol* 82, 275–282.
- 629 Zollikofer CPE, Ponce de León MS (2001) Computer-assisted morphometry of hominoid fossils: the
630 role of morphometric maps. In: *Phylogeny of the Neogene Hominoid Primates of Eurasia*. (eds De
631 Bonis L, Koufos G, Andrews P), pp. 50–59. Cambridge: Cambridge University Press.
- 632 Zollikofer CPE, Ponce de León MS (2005) Virtual Reconstruction: A Primer in Computer-assisted
633 Paleontology and Biomedicine. New York: Wiley.
- 634 Zollikofer CPE, Ponce de León MS (2006) Neanderthals and modern humans—chimps and bonobos:
635 similarities and differences in development and evolution. In: *Neanderthals Revisited: New*
636 *Approaches and Perspectives*. (eds Harvati K, Harrison T), pp. 71–88. New York: Springer.

637 **Tables**

Table 1. Sample structure

Tooth	N (Source ¹)
UM1	62 (Jomon, 8; Medieval, 13; Early modern, 30; Modern, 11)
UM2	54 (Jomon, 31; Modern, 23)
UM3	60 (Jomon, 29; Modern, 31)

¹Jomon (14500–300 BC), Medieval (13–15C AD), Early modern (17–19C AD), and Modern (19C AD–) from Japanese Archipelago (mainland Japanese).

638

Table 2. Morphological differences among 3 maxillary molars

	UM1 versus UM2	UM2 versus UM3	UM1 versus UM3
Mean Shape	1.97***	1.71***	2.30***
Mode of variation	24.64	25.85	24.29***

*** $p < 0.001$.

639

Figure legends

Fig. 1. Variation of human maxillary molars (occlusal view). Specimen IDs correspond to the respective individuals in multivariate shape space (Fig. 3). Specimens #2 and #3 of UM2 exhibit UM1-like and UM3-like morphologies respectively. Scale bar: 5 mm.

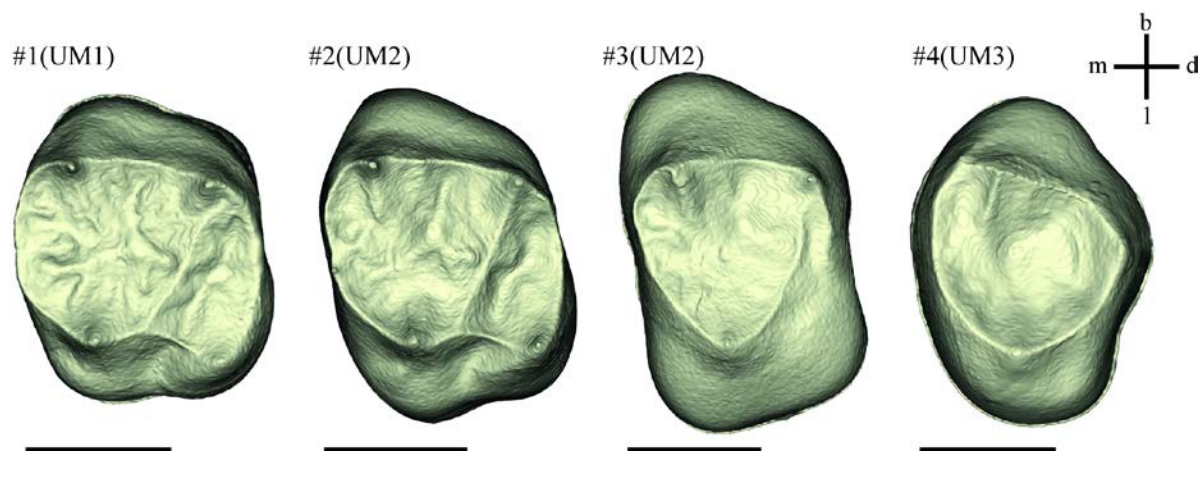
Fig. 2. Scheme of morphometric data sampling and mapping. **(A)** 3D representation of EDJ crown of left UM1 (distal view). Filled circles indicate the digitized cervical line. EDJ is aligned so that the least-squares plane is in accordance with the xy -plane of the Cartesian coordinate system, where its origin is defined by the centroid of the cervical line. **(B)** Sectional view of EDJ. The outline that goes from the centroid to the cervix (d : 0→1) on the section of EDJ surface is parameterized with elliptic Fourier analysis. On this outline, we sampled three variables: c , the mean curvature; h , the height from the cervical plane; and r , the radius from the centroid of the cervical line. **(C)** Three dimensional model of EDJ (occlusal view) that represents the anatomical direction: buccal (0°)→mesial (90°)→lingual (180°)→distal (270°)→buccal (360°). *pa*: paracone; *pr*: protocone; *me*: metacone; *hy*: hypocone; *oc*: oblique crest; *trib*: trigon basin; *tab*: talon basin; *bg*: buccal groove; *lg*: lingual groove; *ca*: Carabelli trait. b: buccal; m: mesial; l: lingual; d: distal. **(D)** Surface topography map (c -M) permits identification of anatomically well-defined features and subtle surface structures. **(E)** Height map (h -M) gives a comprehensive view of the vertical (cusp tip-cervix) dimensions of EDJ, and the relative location and distribution of the cusps. **(F)** Radius map (r -M) represents the extent of the horizontal (parallel to cervical plane) dimensions of EDJ.

Fig. 3. Variation along shape component (SC) 1 and 2 (open circles: UM1, asterisks: UM2, open stars: UM3; large symbols/ellipses indicate tooth-specific means/95%-density ellipses; morphometric maps (c , h , and r , from top to bottom and left to right, respectively) visualizing extreme shapes along each SC axis). Arrow heads indicate increased radius around paracone (paracone protuberance). Arrows correspond to a common allometric vector (allometric vector of the entire sample; black arrow) and an allometric vector for each molar (red arrow: UM1; blue arrow: UM2; green arrow: UM3). The center of

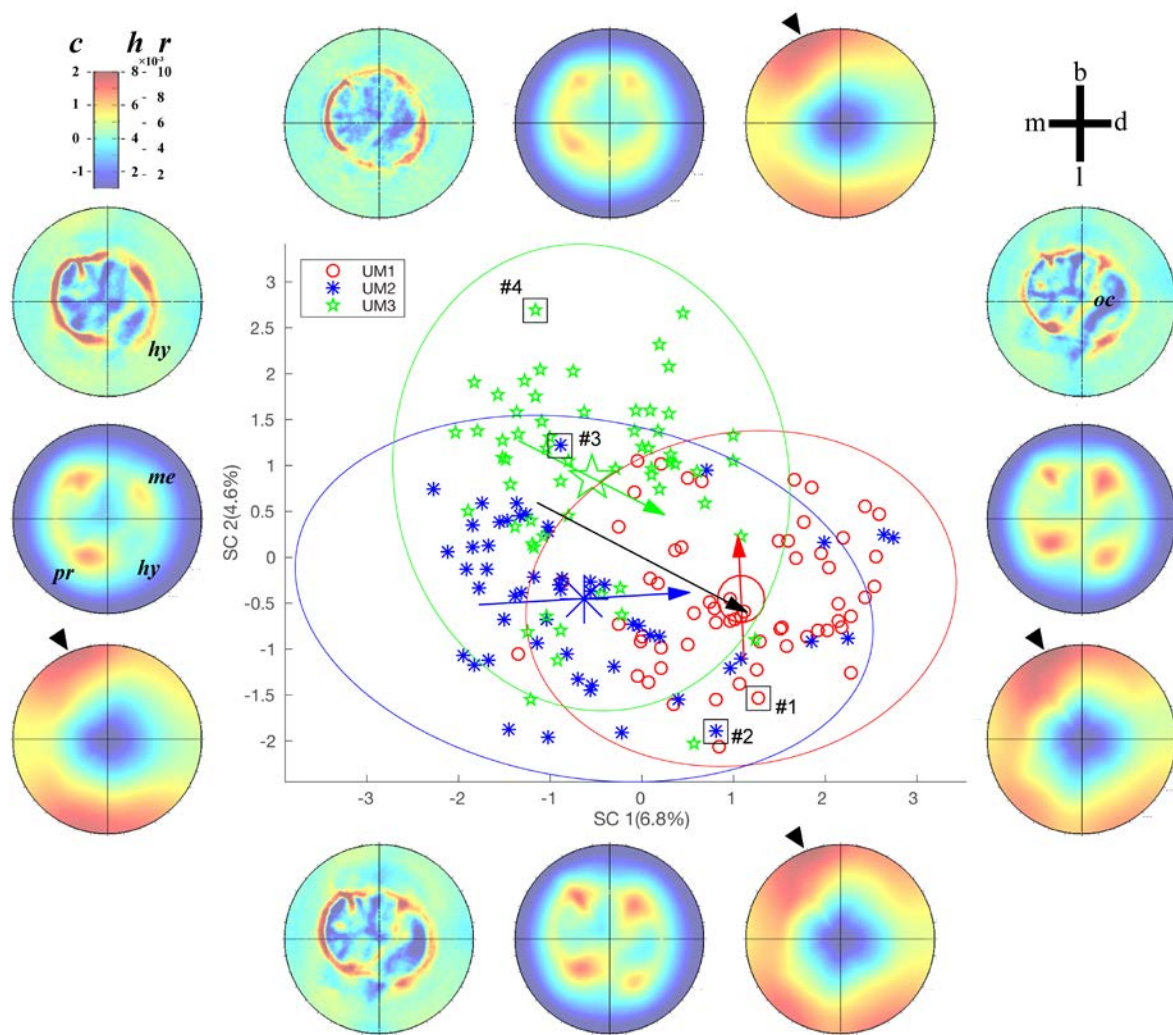
each arrow represents the mean molar shape and the length is defined as twice the standard deviation for the direction of each allometric vector. While the allometric vector of entire sample and that of UM2 show that EDJ morphology approaches UM1 mean shape with increasing size, the allometric vector of UM3 is directed toward relatively large-sized UM1. Specimen IDs correspond to the respective individuals in Fig. 1. *pa*: paracone; *pr*: protocone; *me*: metacone; *hy*: hypocone; *oc*: oblique crest. b: buccal; m: mesial; l: lingual; d: distal. Available in color online.

Fig. 4. Average morphometric maps (*c*, *h*, and *r* from left to right) of each molar (UM1, UM2, and UM3, from top to bottom). Arrow heads indicate increased radius around paracone (paracone protuberance). *pa*: paracone; *pr*: protocone; *me*: metacone; *hy*: hypocone; *oc*: oblique crest; *trib*: trigon basin; *tab*: talon basin; *bg*: buccal groove; *lg*: lingual groove. This figure is also available in color online at [http://onlinelibrary.wiley.com/journal/10.1111/\(ISSN\)1469-7580](http://onlinelibrary.wiley.com/journal/10.1111/(ISSN)1469-7580)

Fig. 5. Comparison of shape variation calculated as the square root of the sum of the squared distances between the mean configuration and each specimen in morphospace. There is a significant difference in the amount of shape variation between UM3 and UM1 or UM2, but not between UM1 and UM2.

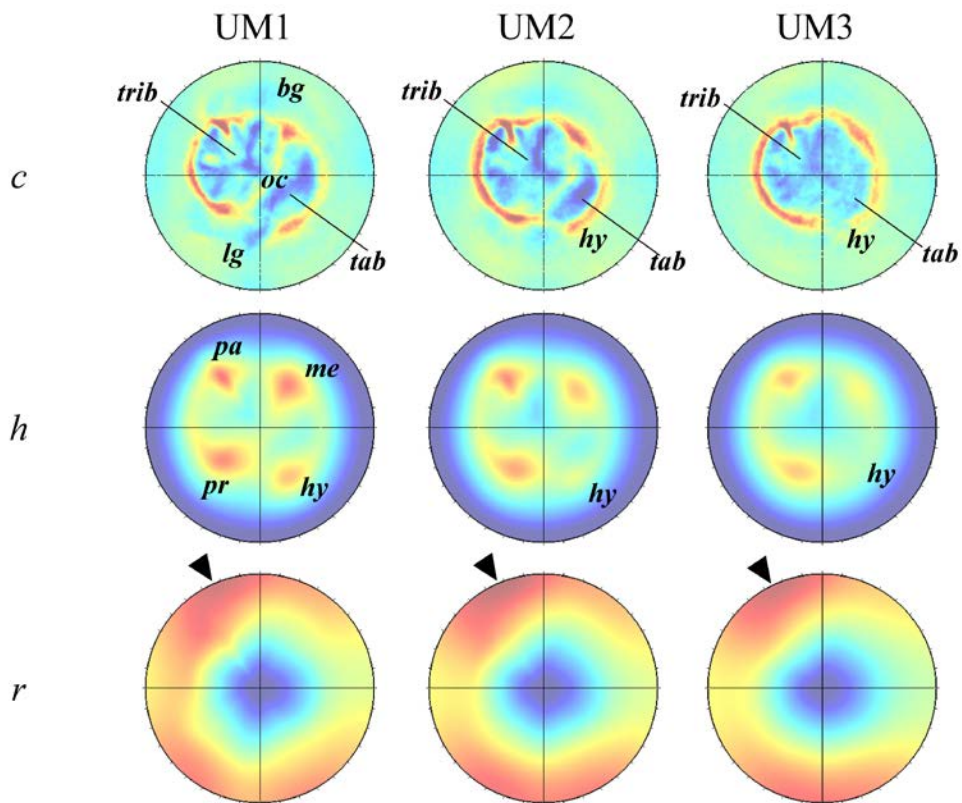






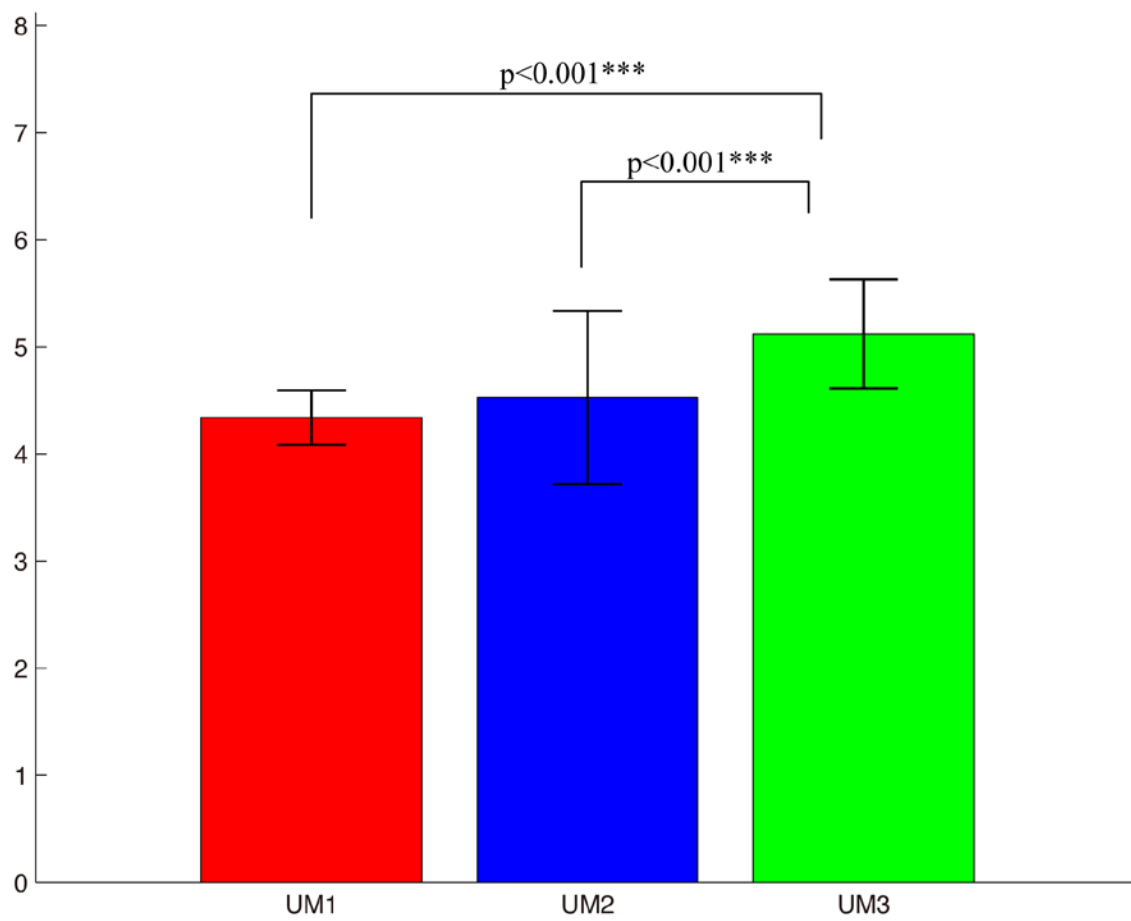
688

689



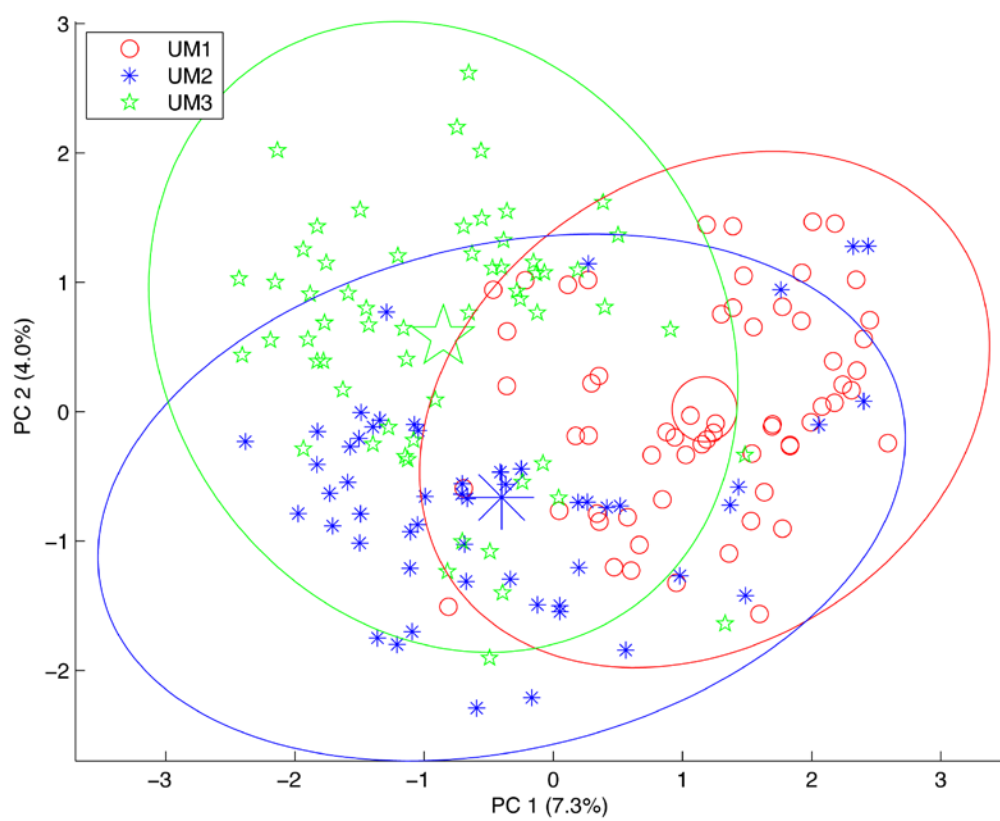
690

691



692

693



694

695

